Section 2

LRF Physics and Model

2.1 Rowland Geometry and Astigmatism

A detailed discussion of the physics of Rowland spectrometers is beyond the scope of this report. What follows is a brief discussion of the basic principles as they apply to the HETGS. Please consult the references for more detailed accounts, including derivation of grating, astigmatism, coma, and aberration equations using Fermat's principle[70], or for specific effects of the faceted grating design.[6]

The HETGS is a simple transmission Rowland spectrometer in which the gratings and detector are located on opposite sides of a Rowland circle. The HETG itself is a faceted Rowland torus design and has been engineered and built to accurately place each facet at its prescribed location and orientation. Although physical-optics analysis of the image produced by this Rowland design can be quite complex[6], the basic features can be understood through simple ray geometry.

In the "Top View" of Figure 2.1 we are looking along the cross-dispersion direction, z'. The diffraction angle is β, as defined by Equation 1.1. Through the geometric properties of the circle, rays diffracted from gratings located along the Rowland circle will all converge at the same diffracted point on the Rowland circle. The dotted lines represent zero-order ($m = 0, \beta = 0$) rays and the solid lines a set of diffracted order ($m > 0, \beta > 0$) rays. The physical distance from zero order to the $m_{\rm th}$ diffracted order, the dispersion distance $D_{\rm disp}$, is given to good approximation by:

$$D_{\rm disp} \approx (\frac{m\frac{hc}{E}}{p})(X_{\rm RS}) = (\frac{m\frac{12.3985}{E_{\rm keV}}}{p})(X_{\rm RS}) \tag{2.1}$$

The bottom panel, "Side View", looks along the dispersion direction, y', at rays from a set of gratings arranged perpendicularly to those above. The grey shaded gratings are the same gratings as visible in the Top View, located on the same Rowland circle, now seen in projection. If the Rowland circle in the Top View is rotated about the dispersion direction axis, it will trace out the additional projected Rowland circles and grating facets shown in the SIde View (black facets). The surface this rotation describes is the *Rowland torus*. Grating facets with their centers located on the torus and their surfaces normal to the converging light rays (dotted lines) will focus diffracted orders on the Rowland circle. Since the Rowland spacing is the same for

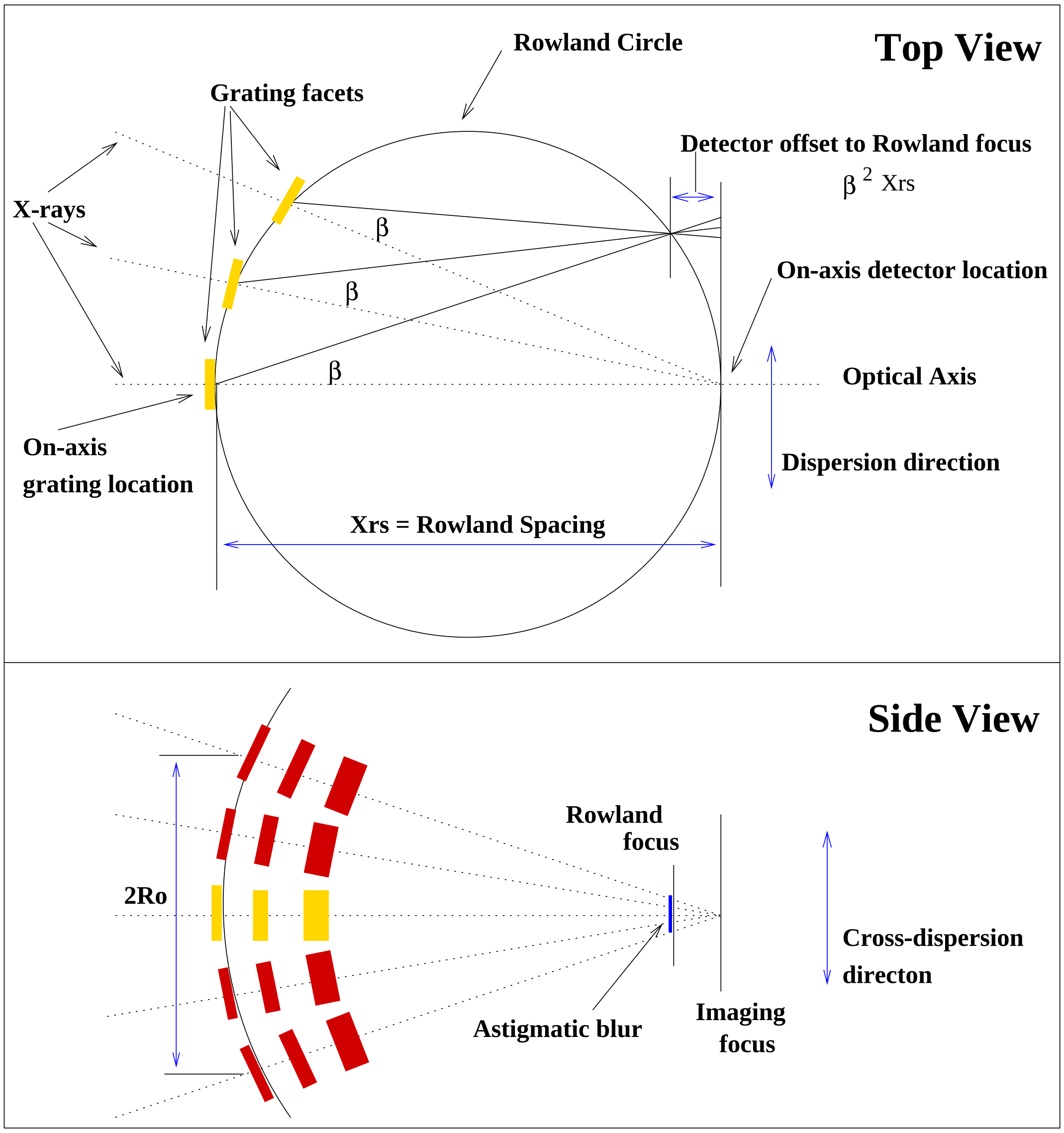

Figure 2.1: Simplified ray geometry for the Rowland torus design. The *Top View* shows the spectrometer layout viewed from +Z ("above AXAF") with the HRMA off the page to the left. X-rays reflected by the HRMA come to a focus at zero order (dotted lines). The grating facets diffract the rays into the m_{th}-order spectra at angle β with respect to the optical axis, and bring the dispersed spectrum to a focus on the Rowland circle (solid lines). The Rowland Spacing, X_{RS}, is the diameter of the Rowland circle and the distance from the gratings to the detector. In the *Side View*, we see the cross-dispersion projection of the same rays. Notice that in the cross-dispersion-direction, the diffracted rays focus behind the Rowland circle.

all grating facets, and the zero order focus coincides for all facets, the m_{th} diffracted order from each facet is focussed at the same angle β, at the same place on the Rowland circle. That is, best focus for the dispersion direction projection occurs along the inner surface of the Rowland torus, which is approximately along the original (horizontal) Rowland circle.

Together, these constructions show the astigmatic nature of the spectrally focussed image: the rays come to a focus in the dispersion direction, the *Rowland focus*, at a different location from their focus in the cross-dispersion direction, the *Imaging focus.* With a detector curved to follow the Rowland focus, diffracted orders or spectral lines are focussed and sharp in the dispersion direction, and elongated in the cross-dispersion direction. The detector offset required to be on the Rowland circle is given by:

$$\Delta X_{\mathrm{Rowland}} = \beta^2 X_{\mathrm{RS}} \tag{2.2}$$

where X_{RS} is the Rowland spacing. In order to maintain the best spectroscopic focus the detector surface must conform to or approximate this Rowland curvature.

At the Rowland focus the image is elongated (blurred) in the cross-dispersion direction by a peak-to-peak value given by similar triangles as:

$$\Delta z' = \frac{2R_0}{X_{\mathrm{RS}}} \Delta X_{\mathrm{Rowland}} \tag{2.3}$$

where R_0 is the perpendicular distance of the ring of gratings from the optical axis.

It is important to note that in the ideal case the grating provides primarily a deflection to the rays being focussed by the HRMA. Because of this, the focus quality is not dramatically effected by perturbations of the grating geometry from the ideal Rowland Torus design. In particular, the flight HETG is built to a Rowland diameter of 8633.69 mm, yet at XRCF because of the finite source distance changes to the HRMA focal length and other considerations, the HETG Rowland spacing (on-axis grating to detector distance) was of order 8800 mm. This difference adds an insignificant additional spectral blur (of order 1 μm rms.)

To-do:
Add ray-trace examples of image formation.
Describe and add ray-trace examples of finite facet blur (small).
Add ray-trace of effect of XRCF mis-positioning.
Check as-installed HETG tilts – need to include in error-budget or **MARX** ?

2.2 LRF Approximation: Resolving Power Error Budget

The LRF of the HETGS can be crudely yet usefully characterized by the location and FWHM of the LRF core in both the dispersion and cross-dispersion directions. The “resolving power” of the spectrometer is defined by:

$$\mathrm{ResolvingPower} = \frac{E}{dE_{\mathrm{FWHM}}} = \frac{y'}{dy'_{\mathrm{FWHM}}} \tag{2.4}$$

The design of the HETG involved the use of an error budget to sum the various contributions to the resolving power. This error budget was useful for studying the dependence of the resolving power on the variation of individual error terms. The error budget results were verified by performing simplified ray-traces of single and multiple facets.

The error budget presented in Table 2.1 includes all of the important error terms for the flight HETGS resolving power; a resulting range of “realistic” curves for the flight HETGS resolving power is plotted as the solid and dashed curves in Figure 2.2.

The error budget terms, their equations, and the current flight value estimates are discussed in the sections below.

To-do:
Describe the “error budget ray-trace” software.

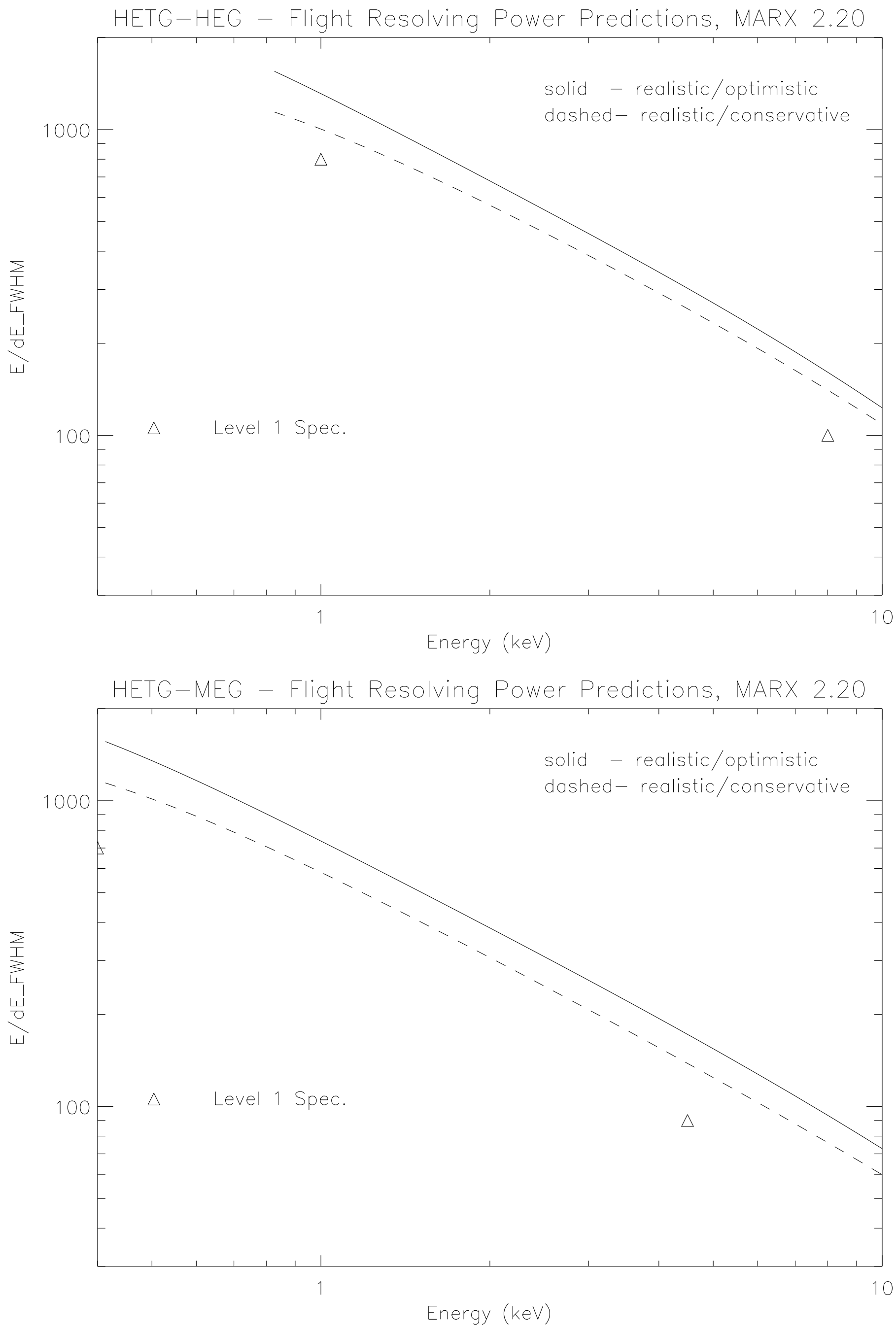

Figure 2.2: Resolving Power for the HEG and MEG spectra of the HETGS plotted vs. energy. The resolving power at high energies is dominated by the HRMA blur; at low energies the grating's effects become important.

The solid and dashed curves are the current range of realistic flight HETGS estimates. The "optimistic" solid curve is calculated from the parameters shown in Table 2.1 and related equations. The dashed curve is the same except for a (plausible) degradation in aspect, focus, and grating dp/p to: $a = 0.6, dx = 0.2, dp/p = 250 \times 10^{-6}$.

Error Term		*Error Parameter*		Blur Equations (rms μm)	
	symbol	value	units	dy',dispersion	dz',cross-disp.
HRMA PSF	$\sigma_{\rm H}$	Equ. 2.7[2.8]	rms mm	$\sigma_{\rm H}$	$\sigma_{\rm H}$
Astigmatism	–			Equ. 2.9	Equ. 2.10
Period var.	dp/p	162[146]	$\times 10^{-6}$ rms	Equ. 2.11	–
Roll var.	γ	1.5	arc min. rms	–	Equ. 2.12
Aspect	a	0.34	arc sec rms	Equ. 2.13	Equ. 2.13
Dither rate	$R_{\rm dither}$	0.1	arc sec./s	Equ. 2.14	Equ. 2.14
Detector	σ_D	0.29×0.024	mm rms	σ_D	σ_D
	Input Parameters				
Energy	E	as desired	keV		
Defocus	dx	0.1	mm		
Readout time	$t_{\rm D}$	3.3	s		
Period	p	4001.[2001.]	Å		
equiv Radius	R_0	470.[330.]	mm		
Rowland spacing	$X_{\rm RS}$	8634.	mm		
Focal length	F	10065.5	mm		
Rowland offset	$\Delta X_{\rm Rowland}$	$\beta^2 X_{\rm RS}$	mm		
Diffr. angle	β	$\arcsin(\lambda/p)$	radians		
Wavelength	λ	hc/E	Å		
hc	hc	12.3985	ÅkeV		

Table 2.1: Simplified Resolving Power Error Budget Equations. The major terms which add blur to the HETG PSF are listed here. The effective rms contributions to the dispersion and cross-dispersion blur are rss'ed together to arrive at a Gaussian approximation to the PSF core in each direction. Note that the equations include unusual factors which convert the values to 1-sigma equivalents, *e.g.*, the rms blur added due to CCD-like pixelization is 0.29 times the pixel size. The parameter values listed here and in the equations are the current best estimates for the flight HETGS. Entries that are different for MEG and HEG are shown as "MEG_value[HEG_value]".

2.2.1 HRMA PSF

The HRMA on-axis, in focus, 1-dimensional projected PSF has a central cusp and extended wings. The result is that the FWHM of this 1-D profile is not a good indicator of the FWHM that will result when convolved with other (generally closer to Gaussian) error terms. In order to parameterize the HRMA for inclusion in this error budget is is useful to measure the "effective HRMA rms blur", σ_H. Define σ_T as the total Gaussian sigma that results from convolving the HRMA 1-D PSF with a Gaussian of width σ_o :

$$\sigma_T = \mathrm{sigma}\{\ \text{HRMA PSF} \ \otimes\ \text{Gaussian}(\sigma_o)\ \} \tag{2.5}$$

then the effective HRMA rms blur is defined as:

$$\sigma_H \ \equiv\ \sqrt{\sigma_T^2 - \sigma_o^2} \tag{2.6}$$

The effective HRMA blur thus depends on the scale at which it is used, σ_o, which is set by the other, non-HRMA, error terms in the error budget.

This procedure was carried out using the approximation to the flight HRMA embodied in the **MARX** software, Version 2.20. The following equations give good approximations to the value of σ_H when $\sigma_o \approx 0.0107\ mm$.

$$\sigma_{H,MEG} = 0.00998\ +\ 0.00014 \log_{10} E\ +\ -0.00399 \log_{10}^2 E\ +\ 0.000505 \log_{10}^3 E \tag{2.7}$$

$$\sigma_{H,HEG} = 0.01134\ +\ 0.00675 \log_{10} E\ +\ -0.01426 \log_{10}^2 E\ +\ 0.01133 \log_{10}^3 E \tag{2.8}$$

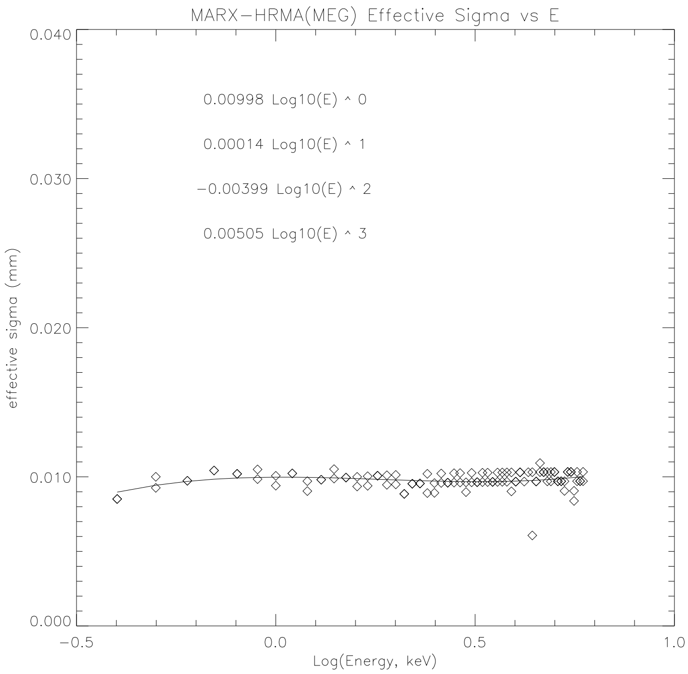

Figure 2.3: Fitting the **MARX** MEG HRMA Effective Blur

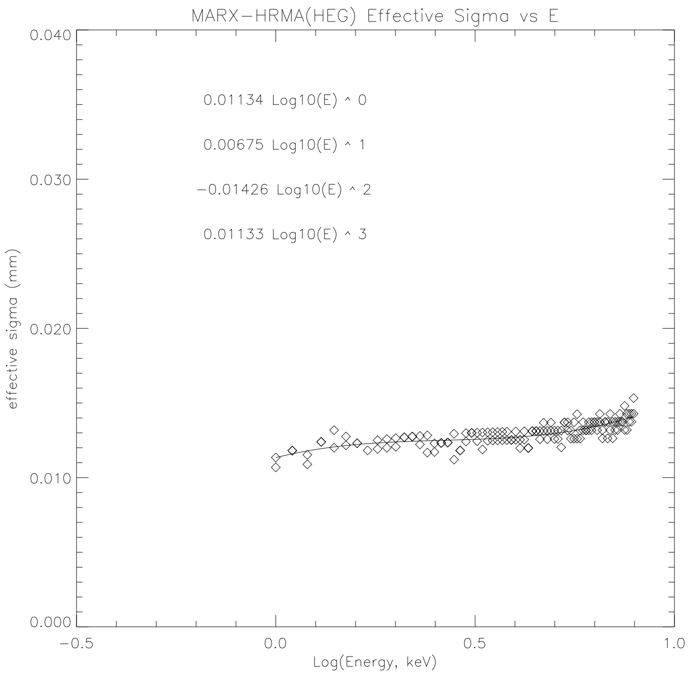

Figure 2.4: Fitting the **MARX** HEG HRMA Effective Blur

2.2.2 Rowland Astigmatism

Including the effect of a defocus, dx, and a factor converting the peak-to-peak blur into an rms equivalent, we get the following equations for the Rowland astigmatism contribution to the error budget:

$$dy' = 0.354 \, \frac{2R_0}{X_{\mathrm{RS}}} \, dx \tag{2.9}$$

$$dz' = 0.354 \, \frac{2R_0}{X_{\mathrm{RS}}} \, (\Delta X_{\mathrm{Rowland}} + dx) \tag{2.10}$$

These equations assume that the detector conforms to the Rowland circle except for an overall translation by dx (positive towards the HRMA). The values of R_0 used in the error budget are effective values – weighted combinations of the relevant mirror shells.

2.2.3 Grating Period and Roll Variations

There are two main error terms which depend on how well the HETG is built: i) period variations within and between facets ("dp/p") and ii) alignment ("roll") variations about the normal to the facet surface within and between facets. The period variations lead to an additional blur in the dispersion direction:

$$dy' \approx \beta X_{\mathrm{RS}} \frac{dp}{p} \tag{2.11}$$

where dy' and dp/p are rms quantities. The roll errors lead to additional blur in the cross-dispersion direction through the equation:

$$dz' \approx \beta X_{\mathrm{RS}} \; \gamma \; (\frac{1}{57.3})(\frac{1}{60}) \tag{2.12}$$

where dz' and γ are rms values in units of mm and arc minutes respectively.

2.2.4 Aspect and Dither Blurs

Aspect reconstruction adds a blur that is currently expected to be $a = 0.34$ arc seconds rms diameter (Aldcroft memo 6/18/97). The resulting one-dimensional rms sigma is thus:

$$dy', dz' = \frac{1}{2}\frac{\sqrt{2}}{2} \;\; F \;\; a \;\; (\frac{1}{57.3})(\frac{1}{3600}) \tag{2.13}$$

where F is the HRMA focal length in mm.

An additional blur is added because the arrival time of a photon at the detector is only known to an accuracy of the detector readout time, t_D. The product of this readout time and the aspect slew rate (basically the dither rate) is the size of the aspect error interval. The rms blur effect is 0.29 times this interval:

$$dy', dz' = 0.29 \;\; F \;\; R_{\text{dither}} \;\; t_D \;\; (\frac{1}{57.3})(\frac{1}{3600}) \tag{2.14}$$

2.2.5 Detector Blur

This error term is the spatial error introduced by the detector readout scheme.

For a pixelated detector like ACIS we assume that the PSF drifts with respect to the detector pixels and there is a uniform distribution of the centroid location in pixel phase. In this case the reported location of an event is the center of the pixel when in fact the event may have actually arrived ± 0.5 pixel from the center. The rms value of such a uniform distribution is 0.29 times the pixel width:

$$\sigma_D = 0.29 \times \text{pixel size} \tag{2.15}$$

For a detector like the HRC, the value σ_D is simply the sigma of the gaussian blur added by the detector.

2.3 Ray-trace Software: MARX

The design of the HETG has required ray-trace software in addition to simple error budgeting. Tom Markert initiated these efforts by using Webster Cash's IRT (interactive Ray-Trace) IDL package. This IRT framework was also used for the "error-budget-ray-trace" work (to be) described in the previous section. In addition, IDL lookup table software (`axaf1.pro`) was developed by the HETG team for effective area studies and simulations. With the addition of ASC personel at MIT these HETG modeling efforts evolved into a pseudo ray-trace IDL code, `sim`, which was then ported to C (`csim`). Because of in-house physics/software expertise (John Davis), `csim` evolved from an error-budget-efficiency combination into a full up ray-trace code. Finally, for release as an ASC product `csim` was renamed **MARX** .

MARX , therefore, is the main HETG ray-trace code and is a joint ASC/HETG effort. It is planned that **MARX** embody all relevant effects for HETGS modeling and simulation. Please see `http://space.mit.edu/ASC/software/software.html` for more information on **MARX** .

2.3.1 XRCF Simulations with MARX

Custom IDL code (`marx/xrcf_sim.pro`) was produced to create modified MARX parameters for a given XRCF measurement. Some items of note in this respect are:

- The modeled spectrum is used as the SpectrumFile with SourceFlux=0.0.
- Generally the ExposureTime is set to 0.0 and the simulation controlled by the NumRays.
- The source distance is set to 537.583 meters; this is the sum of the source-to-HRMA distance, 527.522 meters, and the HRMA-to-infinite-source-focus distance in **MARX** of 10.061 meters.
- A finite source size is modeled with SourceType="DISK" and S-DiskTheta1=0.0959.
- The nominal in-focus detector position is offset to -194.872 mm.
- The MARX grating RowlandDiameter is set to the actual XRCF value minus the 194.872 mm focus offset.
- To better agree with XRCF performance, HRMABlur is set to 0.30 arc seconds.
- The effect of the HXDS axes alignment, Section 5.1.5.1, is included in FPC, SSD, and HSI simulations.
- To simulate the HXDS detectors, the HRC-I is used as the detector for its large, planar field. Additionally HRC-I-BlurSigma=0.0 and DetIdeal="yes".
- The IDL s/w post-processes the simulated events to apply the actual HXDS detector quantum efficiencies.
- The MARX coordinates are flight coordinates and hence are rotated by 180 degrees about the X-axis from the XRCF coordinate system.

`To-do:`
Evaluate the need and method to include HEG scattering in **MARX** .